frontiers | Frontiers in Energy Research

TYPE Original Research
PUBLISHED 12 December 2023
DOI 10.3389/fenrg.2023.1325612

OPEN ACCESS

EDITED BY
Jiangmin Jiang,
China University of Mining and Technology, China

REVIEWED BY
Qiang Chen,
Zhejiang University of Technology, China
Ping Nie,
Jilin Normal University, China

*CORRESPONDENCE
Stefano Passerini,
stefano.passerini@uniroma1.it
Jean-Yves Sanchez,
jeanyves.sanchez@uc3m.es
Dominic Bresser,
dominic.bresser@kit.edu

RECEIVED 21 October 2023
ACCEPTED 30 November 2023
PUBLISHED 12 December 2023

CITATION
Kim G-T, Antonelli C, Iojoiu C, Löffler M, Bresser D, Molméret Y, Sanchez J-Y and Passerini S (2023), Nanocrystalline cellulose reinforced poly(ethylene oxide) electrolytes for lithium-metal batteries with excellent cycling stability.
Front. Energy Res. 11:1325612.
doi: 10.3389/fenrg.2023.1325612

Nanocrystalline cellulose reinforced poly(ethylene oxide) electrolytes for lithium-metal batteries with excellent cycling stability

Guk-Tae Kim[1,2,3], Claire Antonelli[4], Cristina Iojoiu[5,6], Marlou Löffler[1,2], Dominic Bresser[1,2]*, Yannick Molméret[7], Jean-Yves Sanchez[8,9]* and Stefano Passerini[1,2,10]*

[1]Helmholtz Institute Ulm (HIU), Ulm, Germany, [2]Karlsruhe Institute of Technology (KIT), Karlsruhe, Germany, [3]Department of Energy Convergence Engineering, Cheongju University, Cheongju-si, Republic of Korea, [4]Institut Européen des Membranes, IEM-UMR 5635, University Montpellier, ENSCM, CNRS, Montpellier, France, [5]University Grenoble Alpes, University Savoie Mont Blanc, CNRS, Grenoble INP, LEPMI, UMR5279, Grenoble, France, [6]Réseau sur le Stockage Electrochimique de l'Energie (RS2E), CNRS FR3459, Amiens, France, [7]Verkor, Grenoble, France, [8]Materials Science and Engineering Department, University Carlos III of Madrid, Getafe, Spain, [9]University Grenoble Alpes, CNRS, Grenoble INP, LEPMI, Grenoble, France, [10]Chemistry Department, Sapienza University of Rome, Rome, Italy

Polyethylene oxide (PEO) based polymer electrolytes are still the state of the art for commercial lithium-metal batteries (LMBs) despite their remaining challenges such as the limited ionic conductivity at ambient temperature. Accordingly, the realization of thin electrolyte membranes and, thus, higher conductance is even more important, but this requires a sufficiently high mechanical strength. Herein, the incorporation of nanocrystalline cellulose into PEO-based electrolyte membranes is investigated with a specific focus on the electrochemical properties and the compatibility with lithium-metal and $LiFePO_4$-based electrodes. The excellent cycling stability of symmetric Li||Li cells, including the complete stripping of lithium from one electrode to the other, and Li||$LiFePO_4$ cells renders this approach very promising for eventually yielding thin high-performance electrolyte membranes for LMBs.

KEYWORDS

nanocrystalline cellulose, poly(ethylene oxide), polymer, electrolyte, lithium-metal battery

Introduction

Lithium-metal batteries (LMBs) comprising the polymer electrolyte based on polyethylene oxide (PEO) and lithium (trifluoromethanesulfonyl)imide (LiTFSI) and $LiFePO_4$ (LFP) as the cathode have been successfully commercialized more than 20 years ago and deployed as power sources for electric vehicles such as the Bluecar® and the Bluebus® (Zhang and Armand, 2021). An essential criterion for the potential use of such polymer electrolytes is the realization of sufficiently thin and mechanically stable membranes with a suitable ionic conductivity. For dry PEO-based electrolytes, the ionic conductivity commonly reaches practically suitable values in the range of 10^{-3} S cm^{-1} from roughly 70°C, i.e., above the melting temperature of PEO/salt solutions, owing to the enhanced segmental dynamics of the PEO chains favoring the conduction of the lithium

cations (Ratner and Shriver, 1988; Armand, 1990; Ratner et al., 2000; Bresser et al., 2019). Conversely, the mechanical strength decreases at elevated temperatures, rendering the realization of very thin membranes challenging. This is particularly an issue, as the ionic conductance, i.e., the important parameter for the charge transport in the battery cell, depends on the thickness of the polymer membrane–or in other words, the thicker the polymer electrolyte membrane, the lower the conductance. Thus, the mechanical properties of the polymer electrolyte membranes are as essential for a potential commercial exploitation as the ionic conductivity. Common approaches to improve the mechanical strength of PEO-based electrolytes include, for instance, crosslinking the polymer chains (Alloin and Sanchez, 1995; Laik et al., 1998; Kim et al., 2010; Xue et al., 2015; Thiam et al., 2017) or adding inorganic nanoparticles (Appetecchi et al., 1998; Croce et al., 1998; Chung et al., 2001; Ganapatibhotla and Maranas, 2014; Wang and Alexandridis, 2016). Crosslinking, however, commonly results in a reduced ionic conductivity–depending also on the eventual crosslinking density, i.e., the lower the better (Thiam et al., 2017), while the effect of inorganic nanoparticles on the ionic conductivity largely depends on their surface chemistry and acidity, and accordingly on the interaction with the other electrolyte components (Ganapatibhotla and Maranas, 2014; Wang and Alexandridis, 2016). Besides, the addition of relatively large amounts of such inorganic nanoparticles adds a significant weight and volume to the electrolyte membranes, which is detrimental for the energy density of the final battery cell. Although crosslinking is particularly promising in this regard, the need to keep the crosslinking density relatively low in order to not severely impede the charge transport limits the storage modulus to about 1–3 MPa, which is insufficient for realizing very thin membranes (Thiam et al., 2017). An alternative (potentially complementary) approach to yield higher mechanical strength relies on the incorporation of lightweight organic fillers such as microfibrillated cellulose (Chiappone et al., 2011), cellulose nanofibrils (Bobrov et al., 2023), or nanocrystalline cellulose (NCC) (Azizi Samir et al., 2004a; Azizi Samir et al., 2004b; Azizi Samir et al., 2004c; Azizi Samir et al., 2004d; Azizi Samir et al., 2004e). Generally, substantially enhanced storage moduli in the range from 60 to 200 MPa were observed (depending on the eventual amount and electrolyte composition), while the ionic conductivity remained at least comparable to the cellulose-free reference systems (Azizi Samir et al., 2004a; Azizi Samir et al., 2004c; Azizi Samir et al., 2004e; Chiappone et al., 2011). The successful reinforcement of the polymer electrolyte membranes originates from the strong hydrogen-bonding interaction between the NCC, forming a strong network beyond the percolation threshold, which ranges between 1 and 7 wt% depending on the form factor of NCC (El Kissi et al., 2008). Specifically for PEO-NCC nanocomposites, in fact, the formation of such NCC network leads to a Young Modulus between 100 and 600 MPa up to at least 150°C (Sanchez et al., 2016).

Following the in-depth mechanical, physicochemical and electrochemical characterization of NCC-reinforced PEO/LiTFSI polymer electrolytes in previous studies (Azizi Samir et al., 2004a; Azizi Samir et al., 2004b; Azizi Samir et al., 2004c; Azizi Samir et al., 2004d; Azizi Samir et al., 2004e; El Kissi et al., 2008), the herein reported study focuses on the evaluation of this nanocomposite polymer electrolyte systems in symmetric Li||Li cells and Li||LFP cells at varying temperatures to underline the suitability of this approach for realizing the long-term stable cycling of LMBs.

Experimental

Nanocomposite polymer electrolyte preparation

An aqueous suspension of nanocrystalline cellulose (NCC, 2 wt %, FPInnovations) was prepared using a high speed homogenizer, as reported earlier (Azizi Samir et al., 2004b). Poly (ethylene oxide) (PEO; $M_w = 3 \times 10^5$ g mol^{-1}; Sigma-Aldrich) was dissolved in distilled water, resulting in a 3 wt% solution, and the corresponding amount of the aqueous NCC suspension for obtaining a 9:1 ratio (by weight) of PEO and NCC was added. The resulting mixture was vigorously mixed. Subsequently, lithium (trifluoromethane sulfonyl)imide (LiTFSI, Acros Organics) was added to the PEO-NCC dispersion under continuous stirring. The molar ratio was adjusted according to one lithium per 25 ethylene oxide (EO) units, i.e., EO:Li = 25. The resulting homogeneous suspension was slowly frozen in liquid nitrogen prior to its lyophilization. Finally, the PEO-NCC/LiTFSI composite was hot-pressed at 100°C by applying a pressure of 50 kN. The films thus obtained possessed a thickness ranging from 80 to 100 μm and were stored under argon atmosphere.

Physicochemical and thermal characterization

Thermogravimetric analysis (TGA) was performed in oxygen using a TA Instruments Model Q5000 and a Netzsch TG 209 F1 Libra. The samples were hermetically sealed in aluminum pans inside the dry room. The TGA device punched the pans automatically prior to the measurement. After a purge step with O_2, the temperature was ramped (10 K min^{-1}) from room temperature to 600°C. Differential scanning calorimetry (DSC; TA Instruments Discovery, Model Q2000) measurements were performed to determinate the melting and glass transition temperatures. Also in this case, the aluminum crucibles containing the samples were hermetically sealed inside the dry room. The samples were cooled down to −140°C with a temperature ramp of 10 K min^{-1}, followed by a heating step (10 K min^{-1}) up to 140°C. This was repeated for three times, taking into account the second heating step for the further analysis.

Electrochemical characterization

The ionic conductivity was determined by sandwiching the polymer membranes between two metallic copper foils (area: 4 cm^2) assembled in pouch bag-type cells. Impedance spectra were measured using a Solartron 1,260 Frequency Response Analyzer coupled with a Solartron 1,287 Electrochemical Interface. The AC plots were recorded within a temperature

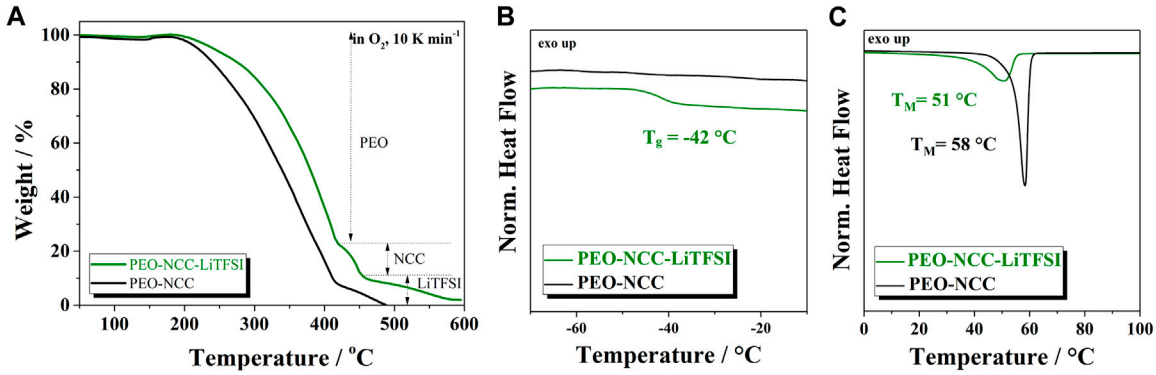

FIGURE 1
(A) Thermogravimetric analysis (TGA) of the NCC-PEO nanocomposite without (in black) and with LiTFSI (in green) as conducting salt as well as differential scanning calorimetry (DSC) measurements in the **(B)** low and **(C)** high temperature region for the determination of the glass transition temperature and melting point, respectively (temperature ramp: 10 K min^{-1}).

range from 10°C to 100°C, applying a frequency range of 100 kHz to 1 Hz and a voltage amplitude of 10 mV. The obtained spectra were fitted using the implemented Z-View® software. For the determination of the electrochemical stability window (ESW) pouch bag-type cells, employing a nickel and a lithium electrode (thickness: 50 µm) were assembled. The measurements were carried out by performing linear sweep voltammetry (LSV) using a Solartron 1,287 potentiostat applying a sweep rate of 0.5 mVs^{-1} and sweeping the cell voltage from the open circuit voltage (OCV). The limiting current density was investigated for symmetrical lithium/lithium cells. The lithium electrodes had a surface area of about 1.4 cm^{-2}. A sweep rate of 0.5 mV s^{-1} was applied using a VMP3 potentiostat (BioLogic) and the evolving current flow was recorded. Similarly, lithium stripping/plating was conducted utilizing symmetrical lithium/lithium cells and applying a constant current density of 0.1 mA cm^{-2} by means of a Maccor 400 battery cycler, reversing the current flow direction every hour. For the complete stripping of one lithium electrode to the other, initially five stripping/plating cycles were carried out before a constant current density was applied for unlimited time until the cell voltage exceeded 2.0 V. For the final full-cell tests, $LiFePO_4$ (LFP, Johnson Matthey Battery Materials) electrodes were prepared by dispersing sodium carboxymethyl cellulose (CMC, Dow Chemical CRT 2000) in deionized water, subsequently adding the conductive carbon (C-NERGY™ Super C45, IMERYS) and LFP and eventually casting the electrode slurry on an aluminum current collector (20 µm, purity >99.9%). The electrodes, having an overall composition of 80:10:10 (LFP:SuperC45:CMC) and average active material mass loading of around 1.6 mg cm^{-2}, were then dried at 140°C overnight under vacuum. In order to fill the electrode pores with an ion-conductive medium, about 25 µL of an ionic liquid-based electrolyte, consisting of LiTFSI dissolved in *N*-butyl-methyl-pyrrolidinium bis(fluorosulfonyl)imide ($PYR_{14}FSI$) in the mole ratio of 1–9 (0.1 LiTFSI-0.9$PYR_{14}FSI$), were placed on the electrode prior to the cell assembly. The resulting cells were dis-/charged galvanostatically using a Maccor 4,000 battery tester within the voltage range from 2.0 to 4.0 V vs. Li^+/Li. A dis-/charge rate of 1C corresponds to a specific current of 170 mA g^{-1}. All herein investigated pouch bag cells were assembled in a dry room, having a relative humidity of less than 0.01% (i.e., a dew point of <60°C). The electrochemical tests were performed at 60°C, if not specified otherwise.

Results and discussion

In a first step, we investigated the thermal properties of the nanocomposite with and without LiTFSI (Figure 1). Both composites were thermally stable up to about 200°C in oxygen atmosphere (Figure 1A), before the temperature-induced mass loss set in. This initial mass loss appears related to the decomposition of PEO, in agreement with previously reported results (Shodai et al., 1994), and accounts for about 90%, thus, confirming the targeted 9:1 ratio of PEO and NCC. At around 400°C, eventually, also the NCC decomposed (Sharma and Varma, 2014; Vanderfleet et al., 2019), which is significantly higher than what had been reported earlier for an NCC nanocomposite with polyvinylidende fluoride (PVdF) (Arbizzani et al., 2014). In the presence of LiTFSI, an additional feature at about 415°C was observed, indicating the degradation of LiTFSI (Zhao et al., 2021). The addition of LiTFSI also enabled the determination of the glass transition temperature (T_g) at about −42°C, which was not observed for the neat PEO-NCC (Figure 1B). This observation is in agreement with a previous study on such nanocomposites (Azizi Samir et al., 2004e). Besides, these findings reveal that the presence of NCC in PEO/LiTFSI has a negligible effect (if any) on the glass transition, since Stolwijk et al. (Stolwijk et al., 2013), for instance, reported a very similar value for PEO/LiTFSI without the NCC. Differently, the addition of LiTFSI led to a slightly lower melting temperature (T_M) of 51°C compared to 58°C for the neat PEO-NCC (Figure 1C), owing to the plasticizing effect of LiTFSI, in particular the $TFSI^-$ anion.

The melting point is also apparent from the plot of the ionic conductivity vs temperature (Figure 2A). In fact, the slope of the temperature-induced increase in conductivity significantly changes between 50°C and 60°C for PEO-NCC/LiTFSI and a little later, i.e., between 60°C and 70°C for PEO-NCC, owing to the change of the pseudo-activation energy when transitioning from the solid to

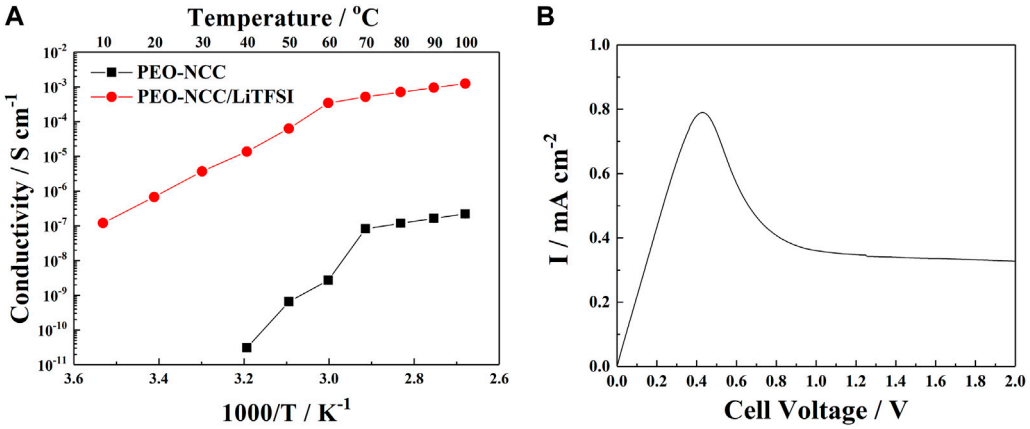

FIGURE 2
(A) Comparative analysis of the ionic conductivity of PEO-NCC (black squares) and LiTFSI-comprising PEO-NCC (red spheres) nanocomposite polymers as a function of temperature. **(B)** Determination of the limiting current density of the LiTFSI-comprising PEO-NCC nanocomposite polymer electrolyte (sweep rate: 0.5 mV s^{-1}; 60°C).

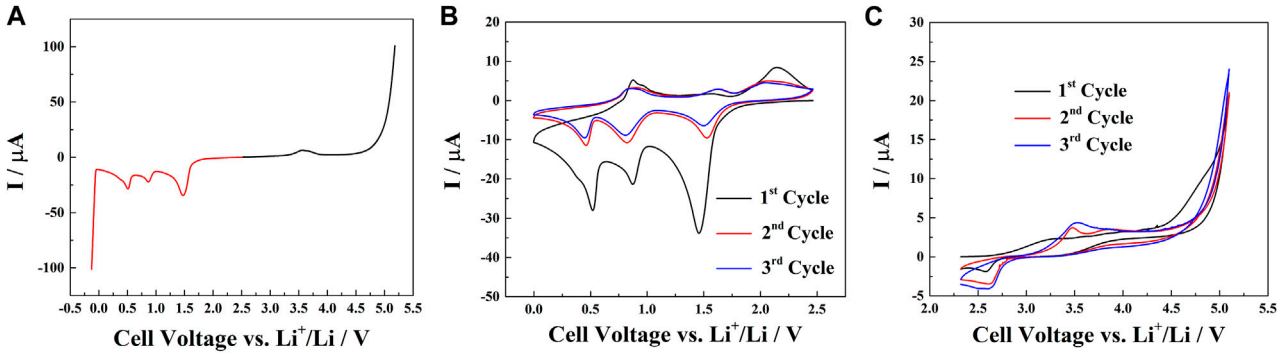

FIGURE 3
Determination of the electrochemical stability window for the PEO-NCC/LiTFSI nanocomposite polymer electrolyte **(A)** by means of linear sweep voltammetry (sweep rate: 0.5 mV s^{-1}; 0–5.0 V; 60°C; cathodic sweep in red and anodic sweep in black) and cyclic voltammetry for the **(B)** low voltage region from 0 to ca. 2.4 V (i.e., OCV) and **(C)** the high voltage region from about 2.4 (i.e., OCV) to 5.0 V–in both cases three cyclic sweeps were conducted.

the molten phase. Generally, the ionic conductivity is in the range from 10^{-4} to 10^{-3} S cm^{-1} between 60°C and 100°C for PEO-NCC/LiTFSI. These values are comparable to NCC-free PEO/LiTFSI electrolytes (Kim et al., 2007), which shows that the addition of NCC has little to no effect on the conductivity. The limiting current density was determined to be about 0.34 mA cm^{-2} at 60°C (Figure 2B), which is about half of the value reported for a ternary electrolyte system comprising PEO, LiTFSI and an ionic liquid (Wetjen et al., 2013), and comparably high for a completely dry electrolyte system.

In a next step, we determined the electrochemical stability window of PEO-NCC/LiTFSI (Figure 3). The linear sweep voltammetry experiments are depicted in Figure 3A, revealing three cathodic peaks at about 1.5, 0.8, and 0.5 V, as well as one rather broad anodic peak at about 3.5 V. The subsequently conducted cyclic voltammetry between 0 and 2.5 V (Figure 3B) showed that these peaks decreased in intensity upon continuous cycling, but did not completely disappear. In fact, there were also three anodic peaks observed, indicating that these processes are related to (quasi-)reversible redox reactions. Earlier studies on PEO/LiTFSI-based electrolyte systems reported very similar findings (Kim et al., 2010; Wetjen et al., 2013) and assigned these features to the reversible reaction of lithium with the NiO_x surface layer on the nickel electrodes (Passerini and Scrosati, 1994). Differently, the cyclic voltammetry experiment performed in the region from OCV (i.e., about 2.3 V) to 5.0 V (Figure 3C) revealed that the anodic peak at about 3.5 V increased in intensity upon cycling. There was no "nearby" cathodic peak that might be related to this anodic peak, but a cathodic feature at about 2.6 V that increased in intensity as well. Given that this was not observed in other PEO-based electrolyte systems, we may assign this to the presence of NCC, potentially a reaction of the remaining hydroxyl groups with lithium that is fairly irreversible with regard to the large peak separation (assuming that these are correlated). Nonetheless, the steep increase in current occurred at about 4.5 V in the first sweep and even higher during the subsequent sweeps, suggesting that the PEO-NCC/LiTFSI

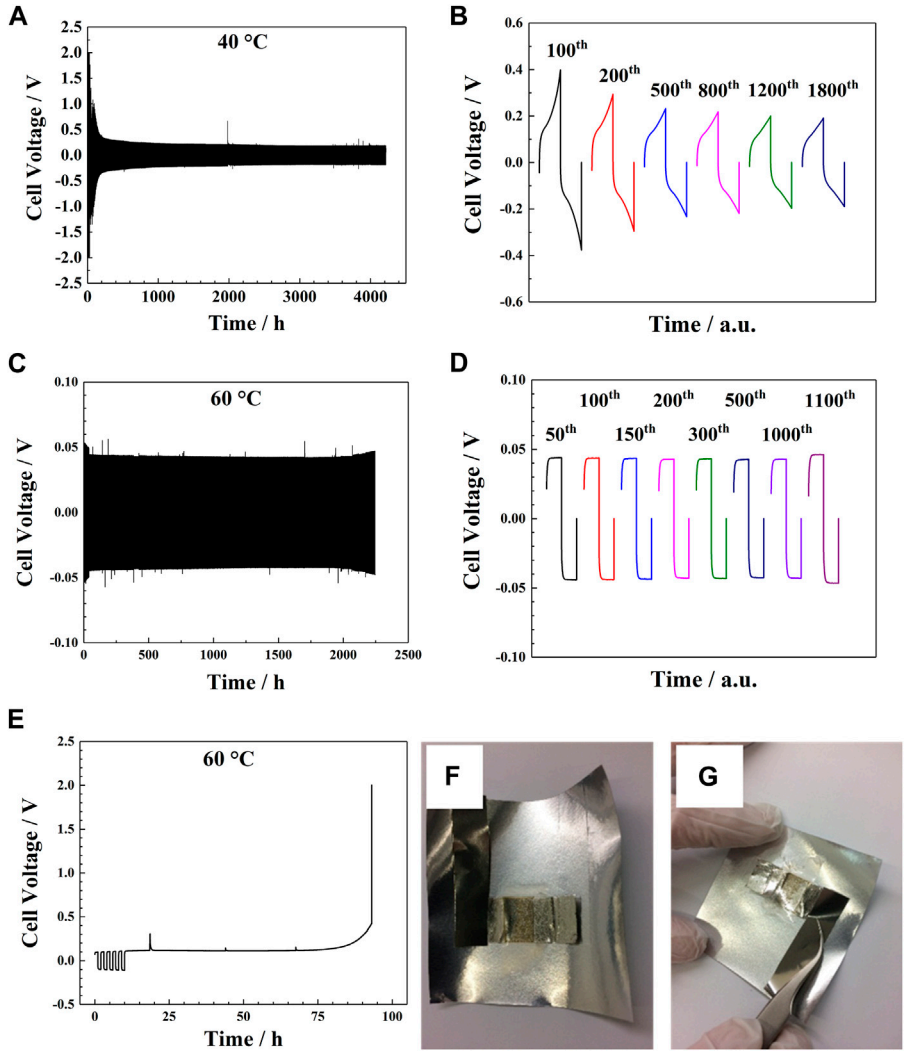

FIGURE 4
Investigation of symmetric Li||Li cells by performing lithium stripping/plating at 40°C **(A)**, including a close-up for selected stripping/plating cycles **(B)**, and at 60°C **(C)**, including as well a close-up of selected stripping/plating cycles **(D)**. In both cases a current density of 0.07 mA cm^{-2} was applied. **(E)** Complete stripping of one lithium electrode and plating it on the counter electrode (60°C; current density: 0.1 mA cm^{-2}) and photographs of the cell opened afterwards in a dry room **(F)** and **(G)**.

nanocomposite electrolyte might be still compatible with LFP cathodes.

First, however, we investigated the compatibility with lithium metal by performing stripping/plating experiments on symmetric Li||Li cells. At 40°C (Figures 4A, B), the cell showed good cycling performance with a stable, though rather high, overpotential of about 0.2 V for more than 4,000 h. The initial decrease in overpotential presumably results from the formation of an apparently beneficial interphase between the nanocomposite electrolyte and the lithium-metal electrodes, a reorganization of the polymer electrolyte at the interface, and an increase in surface area owing to the continuous stripping and plating. The absence of any short circuit, however, indicates that the PEO-NCC/LiTFSI electrolyte system is not prone to dendrite formation. In fact, also when conducting stripping/plating experiments at 60°C (Figures 4C, D), no dendrite formation was observed in the course of the experiment that lasted more than 2,000 h. The overpotential at 60°C was much lower, about 0.045 V, as a result of the substantially higher ionic conductivity (*cf.* Figure 2A) and the initial decrease in overpotential was significantly less pronounced–presumably as any kind of reaction and/or reorganization at the interface, as well as the formation of an interphase is much faster in the liquid-like state. The higher reactivity, though, was also reflected in a slight increase in overpotential after about 2,000 h, indicating an increase of the charge transfer resistance. Nonetheless, the plot of selected stripping/plating profiles in Figure 4D revealed an essentially constant overpotential for each single step, as the applied current density (0.07 mA cm^{-2}) was well below the limiting current density. Remarkably, all the lithium was stripped from one electrode and plated on the other one at a reasonably high current density of 0.1 mA cm^{-2} without any sign of dendrite formation (Figures 4E–G), which further highlights the very good compatibility of the PEO-NCC/LiTFSI electrolyte system with lithium-metal electrodes.

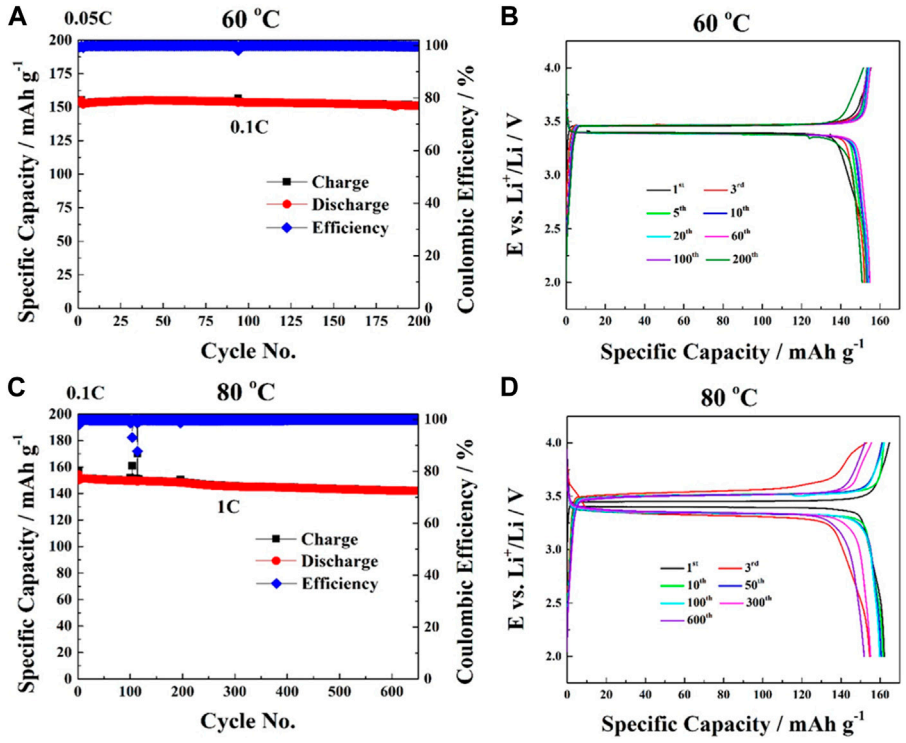

FIGURE 5
(A) Galvanostatic cycling of Li|PEO-NCC/LiTFSI|LFP cells at 60°C (first cycle at 0.05°C and all following cycles at 0.1°C) and **(B)** selected corresponding potential profiles as well as **(C)** at 80°C (first cycle at 0.1°C and all following cycles at 1°C) and **(D)** selected corresponding potential profiles.

Finally, to evaluate the compatibility with LFP-based cathodes, Li|PEO-NCC/LiTFSI|LFP cells were assembled and subjected to galvanostatic cycling experiments at 60°C (Figures 5A, B) and 80°C (Figures 5C, D), since the overpotential is reasonably low at such temperatures as revealed by the stripping/plating experiments conducted in symmetric Li||Li cells. Generally, the cells showed an excellent cycling stability at both temperatures, indicating that the earlier observed redox feature at intermediate potentials (*cf.* Figure 3C) did not have a detrimental impact. More precisely, at 60°C (Figure 5A), the cell delivered a first cycle discharge capacity of 154 mAh g^{-1} at 0.05 C and a first cycle Coulombic efficiency of 99.3%. The Coulombic efficiency subsequently increased to an average value of 99.9% when subjecting the cell to galvanostatic cycling at 0.1C, which is a very high value for a polymer electrolyte and indicates very stable interfaces and interphases at both electrodes. As a result, the capacity retention after 200 cycles at 0.1C was 97.4% based on a reversible specific capacity of 155 mAh g^{-1} in the second cycle and a reversible specific capacity of 151 mAh g^{-1} after 200 cycles. The high stability of the interfaces and interphases was also evident from the comparison of the dis-/charge profiles in Figure 5B, revealing no increase in overpotential and perfectly overlapping voltage plateaus. The length of the voltage plateau, however, slightly decreased upon cycling, suggesting a minor fading of the LFP active material. Similar observations were made at 80°C (Figures 5C, D). The first cycle discharge capacity was essentially the same with about 155 mAh g^{-1} at 0.1C, suggesting that this is the maximum capacity of the LFP active material. The first cycle Coulombic efficiency was slightly lower with around 98.4%, which is assigned to the higher reactivity at such elevated temperature–especially at the interface with the lithium-metal electrode. Subsequently, the Coulombic efficiency increased to an average of 99.8% at 1C, i.e., slightly lower than at 60°C, further corroborating the higher reactivity in this case. Nevertheless, the overall capacity retention was still very high with 94.0% after 667 cycles at 1C based on the reversible specific capacity of 151 mAh g^{-1} in the second cycle and 142 mAh g^{-1} in the 667th cycle. The plot of selected dis-/charge profiles in Figure 5D further corroborated these findings. The voltage plateaus overlap very well initially (despite a slight increase from the first to the following cycles owing to the higher C rate), but get slightly shorter upon cycling, presumably originating from the aforementioned minor fading of the LFP active material. In sum, the Li|PEO-NCC/LiTFSI|LFP cells showed very good cycling stability at 60°C and 80°C, benefiting from stable interfaces and interphases with lithium-metal and LFP electrodes.

Conclusion

The incorporation of nanocrystalline cellulose into PEO/LiTFSI-based polymer electrolytes yields membranes with a suitable ionic conductivity at elevated temperatures above 60°C owing to the melting of the PEO phase, while the high mechanical stability is well preserved. Additionally, the PEO-NCC/LiTFSI electrolyte forms very stable interfaces and interphases with lithium-metal electrodes, enabling the stable cycling of symmetric Li||Li cells for

thousands of hours without any indication of lithium dendrite formation. In fact, even stripping all lithium from one electrode to another does not result in a short circuit of the cells. The overall suitability of this electrolyte system was finally corroborated in Li|| LFP cells, showing very stable cycling for hundreds of cycles at 60°C and 80°C without any increase in polarization and a remarkably high average Coulombic efficiency. These results render the incorporation of lightweight NCC into polymer electrolyte systems a very promising approach to reinforce the corresponding polymer electrolyte membranes, which is essential for achieving thin membranes and, thus, low conductance and, eventually, high energy densities.

Data availability statement

The raw data supporting the conclusions of this article will be made available by the authors, without undue reservation.

Author contributions

G-TK: Data curation, Formal Analysis, Investigation, Methodology, Writing–original draft. CA: Data curation, Investigation, Writing–original draft. CI: Supervision, Writing–review and editing. ML: Data curation, Investigation, Writing–review and editing. DB: Data curation, Funding acquisition, Investigation, Resources, Writing–original draft, Writing–review and editing. YM: Data curation, Investigation, Writing–review and editing. J-YS: Conceptualization, Funding acquisition, Resources, Supervision, Writing–original draft, Writing–review and editing. SP: Conceptualization, Funding acquisition, Resources, Supervision, Writing–review and editing.

Funding

The author(s) declare financial support was received for the research, authorship, and/or publication of this article. The authors would like to acknowledge financial support from the Helmholtz Association and within the FestBatt project (03XP0175B) and the FB2-Poly project (03XP0429B) funded by the German Federal Ministry of Education and Research (BMBF), the National Research Foundation of Korea (NRF) and the Korean government (MSIT, No. RS-2023-00217581), as well as the French National Research Agency (ANR) and KIC InnoEnergy France for their financial support in the framework of the project 'Polymer Electrolyte Nanocomposite for Advanced Lithium Batteries'. Moreover, the authors would like to acknowledge support by the KIT-Publication Fund of the Karlsruhe Institute of Technology (KIT).

Conflict of interest

YM was employed by Verkor.

The remaining authors declare that the research was conducted in the absence of any commercial or financial relationships that could be construed as a potential conflict of interest.

Publisher's note

References

Alloin, F., and Sanchez, J.-Y. (1995). New solvating polyether networks. *Electrochimica Acta* 40, 2269–2276. doi:10.1016/0013-4686(95)00175-E

Appetecchi, G. B., Croce, F., Dautzenberg, G., Mastragostino, M., Ronci, F., Scrosati, B., et al. (1998). Composite polymer electrolytes with improved lithium metal electrode interfacial properties: I. Elechtrochemical properties of dry PEO-LiX systems. *J. Electrochem. Soc.* 145, 4126–4132. doi:10.1149/1.1838925

Arbizzani, C., Colò, F., De Giorgio, F., Guidotti, M., Mastragostino, M., Alloin, F., et al. (2014). A non-conventional fluorinated separator in high-voltage graphite/$LiNi_{0.4}Mn_{1.6}O_4$ cells. *J. Power Sources* 246, 299–304. doi:10.1016/j.jpowsour.2013.07.095

Armand, M. (1990). Polymers with ionic conductivity. *Adv. Mater.* 2, 278–286. doi:10.1002/adma.19900020603

Azizi Samir, M. A. S., Alloin, F., Gorecki, W., Sanchez, J.-Y., and Dufresne, A. (2004a). Nanocomposite polymer electrolytes based on poly(oxyethylene) and cellulose nanocrystals. *J. Phys. Chem. B* 108, 10845–10852. doi:10.1021/jp0494483

Azizi Samir, M. A. S., Alloin, F., Sanchez, J.-Y., and Dufresne, A. (2004b). Cellulose nanocrystals reinforced poly(oxyethylene). *Polymer* 45, 4149–4157. doi:10.1016/j.polymer.2004.03.094

Azizi Samir, M. A. S., Alloin, F., Sanchez, J.-Y., and Dufresne, A. (2004c). Cross-Linked nanocomposite polymer electrolytes reinforced with cellulose whiskers. *Macromolecules* 37, 4839–4844. doi:10.1021/ma049504y

Azizi Samir, M. A. S., Alloin, F., Sanchez, J.-Y., El Kissi, N., and Dufresne, A. (2004d). Preparation of cellulose whiskers reinforced nanocomposites from an organic medium suspension. *Macromolecules* 37, 1386–1393. doi:10.1021/ma030532a

Azizi Samir, M. A. S., Mateos, A. M., Alloin, F., Sanchez, J.-Y., and Dufresne, A. (2004e). Plasticized nanocomposite polymer electrolytes based on poly(oxyethylene) and cellulose whiskers. *Electrochimica Acta* 49, 4667–4677. doi:10.1016/j.electacta.2004.05.021

Bobrov, G., Kedzior, S. A., Pervez, S. A., Govedarica, A., Kloker, G., Fichtner, M., et al. (2023). Coupling particle ordering and spherulitic growth for long-term performance of nanocellulose/poly(ethylene oxide) electrolytes. *ACS Appl. Mater. Interfaces* 15, 1996–2008. doi:10.1021/acsami.2c16402

Bresser, D., Lyonnard, S., Iojoiu, C., Picard, L., and Passerini, S. (2019). Decoupling segmental relaxation and ionic conductivity for lithium-ion polymer electrolytes. *Mol. Syst. Des. Eng.* 4, 779–792. doi:10.1039/c9me00038k

Chiappone, A., Nair, J. R., Gerbaldi, C., Jabbour, L., Bongiovanni, R., Zeno, E., et al. (2011). Microfibrillated cellulose as reinforcement for Li-ion battery polymer electrolytes with excellent mechanical stability. *J. Power Sources* 196, 10280–10288. doi:10.1016/j.jpowsour.2011.07.015

Chung, S. H., Wang, Y., Persi, L., Croce, F., Greenbaum, S. G., Scrosati, B., et al. (2001). Enhancement of ion transport in polymer electrolytes by addition of nanoscale inorganic oxides. *J. Power Sources* 97 (98), 644–648. doi:10.1016/S0378-7753(01)00748-0

Croce, F., Appetecchi, G. B., Persi, L., and Scrosati, B. (1998). Nanocomposite polymer electrolytes for lithium batteries. *Nature* 394, 456–458. doi:10.1038/28818

El Kissi, N., Alloin, F., Dufresne, A., Sanchez, J., Bossard, F., D'Aprea, A., et al. (2008). Influence of cellulose nanofillers on the rheological properties of polymer electrolytes. *AIP Conf. Proc.* 1027, 87–89. doi:10.1063/1.2964880

Ganapatibhotla, L. V. N. R., and Maranas, J. K. (2014). Interplay of surface chemistry and ion content in nanoparticle-filled solid polymer electrolytes. *Macromolecules* 47, 3625–3634. doi:10.1021/ma500072j

Kim, G.-T., Appetecchi, G. B., Alessandrini, F., and Passerini, S. (2007). Solvent-free, PYR_{1A}TFSI ionic liquid-based ternary polymer electrolyte systems: I. Electrochemical characterization. *J. Power Sources* 171, 861–869. doi:10.1016/j.jpowsour.2007.07.020

Kim, G. T., Appetecchi, G. B., Carewska, M., Joost, M., Balducci, A., Winter, M., et al. (2010). UV cross-linked, lithium-conducting ternary polymer electrolytes containing ionic liquids. *J. Power Sources* 195, 6130–6137. doi:10.1016/j.jpowsour.2009.10.079

Laik, B., Legrand, L., Chausse, A., and Messina, R. (1998). Ion–ion interactions and lithium stability in a crosslinked PEO containing lithium salts. *Electrochimica Acta* 44, 773–780. doi:10.1016/S0013-4686(98)00247-3

Passerini, S., and Scrosati, B. (1994). Characterization of nonstoichiometric nickel oxide thin-film electrodes. *J. Electrochem. Soc.* 141, 889–895. doi:10.1149/1.2054853

Ratner, M. A., Johansson, P., and Shriver, D. F. (2000). Polymer electrolytes: ionic transport mechanisms and relaxation coupling. *MRS Bull.* 25, 31–37. doi:10.1557/mrs2000.16

Ratner, M. A., and Shriver, D. F. (1988). Ion transport in solvent-free polymers. *Chem. Rev.* 88, 109–124. doi:10.1021/cr00083a006

Sanchez, J.-Y., Iojoiu, C., Molmeret, Y., and Antonelli, C. (2016). *Ionically conductive material for electrochemical generator and production methods*.

Sharma, P. R., and Varma, A. J. (2014). Thermal stability of cellulose and their nanoparticles: effect of incremental increases in carboxyl and aldehyde groups. *Carbohydr. Polym.* 114, 339–343. doi:10.1016/j.carbpol.2014.08.032

Shodai, T., Owens, B. B., Ohtsuka, H., and Yamaki, J. (1994). Thermal stability of the polymer electrolyte $(PEO)_8LiCF_3SO_3$. *J. Electrochem. Soc.* 141, 2978–2981. doi:10.1149/1.2059268

Stolwijk, N. A., Heddier, C., Reschke, M., Wiencierz, M., Bokeloh, J., and Wilde, G. (2013). Salt-concentration dependence of the glass transition temperature in PEO–NaI and PEO–LiTFSI polymer electrolytes. *Macromolecules* 46, 8580–8588. doi:10.1021/ma401686r

Thiam, A., Antonelli, C., Iojoiu, C., Alloin, F., and Sanchez, J.-Y. (2017). Optimizing ionic conduction of poly(oxyethylene) electrolytes through controlling the cross-link density. *Electrochimica Acta* 240, 307–315. doi:10.1016/j.electacta.2017.04.046

Vanderfleet, O. M., Reid, M. S., Bras, J., Heux, L., Godoy-Vargas, J., Panga, M. K. R., et al. (2019). Insight into thermal stability of cellulose nanocrystals from new hydrolysis methods with acid blends. *Cellulose* 26, 507–528. doi:10.1007/s10570-018-2175-7

Wang, W., and Alexandridis, P. (2016). Composite polymer electrolytes: nanoparticles affect structure and properties. *Polymers* 8, 387. doi:10.3390/polym8110387

Wetjen, M., Kim, G.-T., Joost, M., Winter, M., and Passerini, S. (2013). Temperature dependence of electrochemical properties of cross-linked poly(ethylene oxide)–lithium bis(trifluoromethanesulfonyl)imide–N-butyl-N-methylpyrrolidinium bis(trifluoromethanesulfonyl)imide solid polymer electrolytes for lithium batteries. *Electrochimica Acta* 87, 779–787. doi:10.1016/j.electacta.2012.09.034

Xue, Z., He, D., and Xie, X. (2015). Poly(ethylene oxide)-based electrolytes for lithium-ion batteries. *J. Mater. Chem. A* 3, 19218–19253. doi:10.1039/C5TA03471J

Zhang, H., and Armand, M. (2021). History of solid polymer electrolyte-based solid-state lithium metal batteries: a personal account. *Isr. J. Chem.* 61, 94–100. doi:10.1002/ijch.202000066

Zhao, L., Inoishi, A., and Okada, S. (2021). Thermal risk evaluation of concentrated electrolytes for Li-ion batteries. *J. Power Sources Adv.* 12, 100079. doi:10.1016/j.powera.2021.100079